

Stripes in the extended $t - t'$ Hubbard model: A Variational Monte Carlo analysis

Vito Marino^{1,3}, Federico Becca², Luca F. Tocchio^{3*}

1 Dipartimento di Fisica, Università di Torino, Via P. Giuria 1, I-10125 Torino, Italy.

2 Dipartimento di Fisica, Università di Trieste, Strada Costiera 11, I-34151 Trieste, Italy

3 Institute for Condensed Matter Physics and Complex Systems, DISAT, Politecnico di Torino, I-10129 Torino, Italy

* luca.tocchio@polito.it

December 1, 2021

Abstract

By using variational quantum Monte Carlo techniques, we investigate the instauration of stripes (i.e., charge and spin inhomogeneities) in the Hubbard model on the square lattice at hole doping $\delta = 1/8$, with both nearest- (t) and next-nearest-neighbor hopping (t'). Stripes with different wavelengths λ (denoting the periodicity of the charge inhomogeneity) are stabilized for sufficiently large values of the electron-electron interaction U/t . The general trend is that λ increases going from negative to positive values of t'/t and decreases by increasing U/t . In particular, the $\lambda = 8$ stripe obtained for $t' = 0$ and $U/t = 8$ [L.F. Tocchio, A. Montorsi, and F. Becca, *SciPost Phys.* **7**, 21 (2019)] shrinks to $\lambda = 6$ for $U/t \gtrsim 10$. The latter value of the stripe wavelength is found to be stable in a large region of the phase diagram, within the $(t'/t, U/t)$ plane. For $U/t = 8$ and positive values of t'/t , stripes with wavelength $\lambda = 12$ and $\lambda = 16$ are also obtained, while, for $U/t = 12$ and negative t'/t , the state with $\lambda = 4$ can be stabilized. In all these cases, pair-pair correlations are highly suppressed with respect to the uniform state (obtained for large values of $|t'/t|$), suggesting that striped states are not superconducting at $\delta = 1/8$.

Contents

1	Introduction	2
2	Variational Monte Carlo method	4
3	Results	5
	3.1 Varying U/t with $t' = 0$	6
	3.2 Varying t'/t with $U/t = 8$ and 12	8
4	Conclusions	11
	References	14

1 Introduction

Since the first experimental evidence of superconductivity in copper-oxide materials [1], high-temperature cuprate superconductors attracted a lot of interest, both for the potential applications and for the mysteries in their theoretical description [2, 3]. Among many unsolved questions, there is the interplay between superconductivity and charge and spin inhomogeneities, which have been dubbed *stripes* [4]. Indeed, the possibility that cuprate superconductors may be on the verge of charge and/or spin instabilities has been suggested not long after their discovery [5, 6]. A strong signature for spin inhomogeneities came from neutron scattering measurements in $\text{La}_{1.48}\text{Nd}_{0.4}\text{Sr}_{0.12}\text{CuO}_4$ [7]. Since then, a variety of experimental probes pointed to the presence of spin or charge orders [8–12]. Recently, charge-density fluctuations with short correlation lengths have been shown to be present in a wide region of the temperature-doping phase diagram [13, 14]. Still, the implication of stripes in the insurgence of superconductivity is not clear. For example, $\text{La}_{2-x}\text{Ba}_x\text{CuO}_4$ exhibits a sharp depression in the superconducting transition temperature around $x = 1/8$, while $\text{La}_{2-x}\text{Sr}_x\text{CuO}_4$ shows only a small kink at the same electron density. The only difference between the two compounds is the structural phase transition that occurs at low temperatures when Ba is present [15–17].

The simplest model that has been considered to reproduce the essential features of the cuprates' phase diagram is the single-band Hubbard model on the square lattice, which is characterized by the nearest-neighbor hopping t and the on-site electron-electron repulsion U . Unfortunately, obtaining exact solutions or even accurate approximations for the ground state and for low-energy excitations is far from being trivial. In the recent past, several states have been proposed, being very close in energy, and different conclusions have been obtained by various numerical and analytical methods [18]. The search for the absolute energy minimum represents a formidable task, especially for the relevant electron densities that are expected to give rise to unconventional superconductivity. In this respect, it is important to assess the role of additional parameters, in enhancing the tendency towards superconductivity or stripes. For that, here we consider the extended Hubbard model that includes the next-nearest-neighbor hopping t' :

$$\mathcal{H} = -t \sum_{\langle R,R' \rangle, \sigma} c_{R,\sigma}^\dagger c_{R',\sigma} - t' \sum_{\langle\langle R,R' \rangle\rangle, \sigma} c_{R,\sigma}^\dagger c_{R',\sigma} + \text{H.c.} + U \sum_R n_{R,\uparrow} n_{R,\downarrow}, \quad (1)$$

where $c_{R,\sigma}^\dagger$ ($c_{R,\sigma}$) creates (destroys) an electron with spin σ on site R and $n_{R,\sigma} = c_{R,\sigma}^\dagger c_{R,\sigma}$ is the electron density per spin σ on site R . In the following, we indicate the coordinates of the sites with $\mathbf{R} = (x, y)$. The nearest- and next-nearest-neighbor hoppings are denoted by t and t' , respectively, while U is the on-site Coulomb interaction. The electron density is given by $n = N/L$, where N is the number of electrons and L is the total number of sites. The hole doping is defined as $\delta = 1 - n$.

The presence of stripes in the Hubbard model has been first proposed by using density-matrix renormalization group (DMRG) on 6-leg ladders for the case with $t' = 0$ [19, 20]. Then, further investigations supported the idea that charge and spin inhomogeneities may pervade

the phase diagram of the Hubbard model [21, 22]. In this context, a recent work [23], which combined a variety of numerical techniques, focused on the representative doping $\delta = 1/8$ and $U/t = 8$. Here, the existence of stripes with different lengths has been reported, the lowest-energy stripe being a bond-centered one with periodicity $\lambda = 8$ in the charge sector and $2\lambda = 16$ in the spin sector. As a consequence, the enlarged unit cell of length λ contains, on average, one hole, as obtained by previous Hartree-Fock calculations [24–27]. Still, different wavelengths (from $\lambda = 5$ to 8) were found very close in energy in Ref. [23]. Electron pairing was not found for $\lambda = 8$, but it was detected at other wavelengths. In addition, further studies, based on variational Monte Carlo [28], variational auxiliary-field Monte Carlo [29] and a combination of constrained-path auxiliary field Monte Carlo and DMRG [30], highlighted the absence of superconductivity at doping $1/8$, the system being possibly an insulator.

The presence of stripes away from $\delta = 1/8$ has been investigated by cellular dynamical mean-field theory [31] and variational Monte Carlo approaches [28, 32]. In particular, superconductivity is proposed to coexist with stripes, with the remarkable exceptions for $\delta = 1/8$ and $\delta = 1/6$ [28]. Still, recent calculations based on variational auxiliary-field Monte Carlo, cast a doubt on this coexistence, suggesting that a large region of phase separation may occur as a function of doping [29]. Besides these works, it is important to investigate the effect of a next-nearest neighbor hopping, that is present in all the materials of the cuprate family [33]. Quantum Monte Carlo calculations [34, 35] suggested that the length of the stripe is reduced in presence of a negative next-nearest-neighbor hopping t' . In addition, an extensive study based on the projected entangled-pair states indicated that the half-filled stripe with $\lambda = 4$ is present for $-0.4 \lesssim t'/t \lesssim -0.1$ [36]. Concomitant superconductivity is not present at $\delta = 1/8$ and appears only for larger doping values. Conversely, on the 4-leg ladder, DMRG calculations reported a completely different picture, where the presence of the next-nearest neighbor hopping drives the system to have both superconducting and charge correlations that decay as a power law, while spin correlations decay exponentially [37, 38]. However, the 4-leg ladder may be a peculiar geometry, where, for example, ordinary d -wave pairing is replaced by a plaquette pairing [39].

In this work, we employ the variational Monte Carlo method with backflow correlations to investigate the effect of the next-nearest neighbor hopping t' and of the Coulomb repulsion U on the presence of stripes and superconductivity at doping $1/8$. Our simulations are performed on ladder systems, with L_y legs and L_x rungs, the total number of sites being $L = L_x \times L_y$. In particular, we focus on a 6-leg cylinder geometry, that has been employed in DMRG calculations and is expected to capture the properties of truly two-dimensional clusters [23], while it allows us to accommodate long stripes along the rungs. We have also verified in selected cases that stripes are stable when working directly in two dimensions. First, we fix $t' = 0$ and vary U . Here, the ground state changes from a uniform metal (at low values of the Coulomb repulsion) to an insulator with an optimal stripe of wavelength $\lambda = 8$ and eventually becomes a striped metal with $\lambda = 6$. Then, we analyze the effect of the next-nearest-neighbor hopping for two values of the electron-electron interaction $U/t = 8$ and 12. The general feature is that a negative (positive) ratio t'/t tends to reduce (increase) the length of the stripe, until a uniform state is obtained for large values of $|t'/t|$ (with Néel order for $t'/t > 0$). For $U/t = 8$ stripes with wavelength 12 and 16 are detected between $\lambda = 8$ and the uniform state, while for $U/t = 12$ a direct transition between these states is observed. For $U/t = 12$, a stripe with $\lambda = 4$ is found for negative values of t'/t , in the vicinity of the uniform state. Superconducting correlations are strongly suppressed when stripes are present, indicating that $\delta = 1/8$ is not superconducting for whatsoever stripe wavelengths.

2 Variational Monte Carlo method

Our numerical results are based upon the definition of suitable correlated variational wave functions, whose physical properties can be evaluated within Monte Carlo techniques [40]. In particular, electron-electron correlation is inserted by means of the so-called Jastrow factor [41, 42] on top of a Slater determinant or a Bardeen-Cooper-Schrieffer (BCS) state. In addition, backflow correlations, as described in Refs. [43, 44], are implemented. The latter ingredient is important to get accurate variational states, whose accuracy is comparable to other state-of-the-art numerical approaches [45]. Our simulations are performed on ladders with $L = L_x \times 6$ sites and periodic boundary conditions along both the x and the y directions. In order to fit charge and spin patterns in the cluster, we take $L_x = 2k\lambda$ (with k integer).

The wave function is defined by:

$$|\Psi\rangle = \mathcal{J}_d |\Phi_0\rangle, \quad (2)$$

where \mathcal{J}_d is the density-density Jastrow factor and $|\Phi_0\rangle$ is a state that is constructed from the ground state of an auxiliary noninteracting Hamiltonian by applying backflow correlations [43, 44].

The Jastrow factor is given by

$$\mathcal{J}_d = \exp\left(-\frac{1}{2} \sum_{R,R'} v_{R,R'} n_R n_{R'}\right), \quad (3)$$

where $n_R = \sum_{\sigma} n_{R,\sigma}$ is the electron density on site R and $v_{R,R'}$ are pseudopotentials that are optimized for every independent distance $|\mathbf{R} - \mathbf{R}'|$ of the lattice.

The auxiliary noninteracting Hamiltonian includes different terms:

$$\mathcal{H}_{\text{aux}} = \mathcal{H}_0 + \mathcal{H}_{\text{charge}} + \mathcal{H}_{\text{spin}} + \mathcal{H}_{\text{AF}} + \mathcal{H}_{\text{BCS}}. \quad (4)$$

The first one defines the kinetic energy of the electrons:

$$\mathcal{H}_0 = -t \sum_{\langle R,R'\rangle, \sigma} c_{R,\sigma}^{\dagger} c_{R',\sigma} - \tilde{t}' \sum_{\langle\langle R,R'\rangle\rangle, \sigma} c_{R,\sigma}^{\dagger} c_{R',\sigma} + \text{H.c.}, \quad (5)$$

where the value of the nearest neighbor hopping parameter t is fixed to be equal to the one in the Hubbard Hamiltonian of Eq. (1), in order to set the energy scale. Then, the second and third terms describe bond-centered striped states:

$$\mathcal{H}_{\text{charge}} = \Delta_c \sum_R \cos\left[Q\left(x - \frac{1}{2}\right)\right] \left(c_{R,\uparrow}^{\dagger} c_{R,\uparrow} + c_{R,\downarrow}^{\dagger} c_{R,\downarrow}\right), \quad (6)$$

and

$$\mathcal{H}_{\text{spin}} = \Delta_s \sum_R (-1)^{x+y} \sin\left[\frac{Q}{2}\left(x - \frac{1}{2}\right)\right] \left(c_{R,\uparrow}^{\dagger} c_{R,\uparrow} - c_{R,\downarrow}^{\dagger} c_{R,\downarrow}\right); \quad (7)$$

here, charge and spin modulations (in the x direction) have periodicity $\lambda = 2\pi/Q$ and $2\lambda = 4\pi/Q$, respectively, while Néel order is assumed along the y direction. In addition, a standard Néel order with pitch vector $\mathbf{K} = (\pi, \pi)$ can be considered, as the fourth term in Eq. (4):

$$\mathcal{H}_{\text{AF}} = \Delta_{\text{AF}} \sum_R (-1)^{x+y} \left(c_{R,\uparrow}^{\dagger} c_{R,\uparrow} - c_{R,\downarrow}^{\dagger} c_{R,\downarrow}\right). \quad (8)$$

Finally, the last term induces electron pairing:

$$\mathcal{H}_{\text{BCS}} = \sum_{R,\eta=x,y} \Delta_{R,R+\eta} (c_{R,\uparrow}^\dagger c_{R+\eta,\downarrow}^\dagger - c_{R,\downarrow}^\dagger c_{R+\eta,\uparrow}^\dagger) + \text{H.c.} - \mu \sum_{R,\sigma} c_{R,\sigma}^\dagger c_{R,\sigma}, \quad (9)$$

where the pairing amplitude may also be modulated in real space:

$$\Delta_{R,R+x} = \Delta_x \left| \cos \left[\frac{Q}{2} x \right] \right| \quad \Delta_{R,R+y} = -\Delta_y \left| \cos \left[\frac{Q}{2} \left(x - \frac{1}{2} \right) \right] \right|. \quad (10)$$

This modulation has been named ‘‘in phase’’ in Ref. [46]. Alternatively a uniform pairing amplitude (with d -wave symmetry) can be considered, corresponding to $Q = 0$; a fictitious chemical potential μ is also included in \mathcal{H}_{BCS} .

The auxiliary Hamiltonian of Eq. (4) can be diagonalized by standard methods. Its ground state is then constructed. On top of it, backflow correlations are inserted to define $|\Phi_0\rangle$ of Eq. (2), following our previous works [43,44].

The optimizations of the variational wave function are performed by imposing either $\Delta_{\text{AF}} = 0$, fixing a given stripe wavelength λ , and optimizing Δ_x , Δ_y , μ , Δ_c , Δ_s , and \tilde{t}' (as well as all the pseudopotentials in the Jastrow factor and the backflow parameters) or imposing $\Delta_c = \Delta_s = 0$ and a uniform pairing, optimizing all the other parameters. In the former case, we will denote the resulting wave function as ‘‘striped state’’; in the latter one we will denote it as ‘‘uniform state’’ (even if Néel order can be present, whenever $\Delta_{\text{AF}} \neq 0$).

In order to unveil the presence of charge and spin inhomogeneities, we compute static structure factors:

$$N(\mathbf{q}) = \frac{1}{L} \sum_{R,R'} \langle n_R n_{R'} \rangle e^{i\mathbf{q}\cdot(\mathbf{R}-\mathbf{R}')}, \quad (11)$$

and

$$S(\mathbf{q}) = \frac{1}{L} \sum_{R,R'} \langle S_R^z S_{R'}^z \rangle e^{i\mathbf{q}\cdot(\mathbf{R}-\mathbf{R}')}, \quad (12)$$

where $\langle \dots \rangle$ indicates the expectation value over the variational wave function and $S_R^z = 1/2(c_{R,\uparrow}^\dagger c_{R,\uparrow} - c_{R,\downarrow}^\dagger c_{R,\downarrow})$. The presence of a peak (diverging in the thermodynamic limit) at a given \mathbf{q} vector denotes the presence of charge order in the system. Moreover, the small- q behavior of $N(\mathbf{q})$ allows us to assess the metallic or insulating nature of the ground state. Indeed, charge excitations are gapless when $N(\mathbf{q}) \propto |\mathbf{q}|$ for $|\mathbf{q}| \rightarrow 0$, while a charge gap is present whenever $N(\mathbf{q}) \propto |\mathbf{q}|^2$ for $|\mathbf{q}| \rightarrow 0$ [44,47].

The possible existence of superconductivity is investigated by computing correlation functions between Cooper pairs at distance r . In particular, we can consider pairs along the y direction, so that:

$$D(r) = \left\langle \left(c_{R,\uparrow}^\dagger c_{R+y,\downarrow}^\dagger - c_{R,\downarrow}^\dagger c_{R+y,\uparrow}^\dagger \right) \left(c_{R',\uparrow}^\dagger c_{R'+y,\downarrow}^\dagger - c_{R',\downarrow}^\dagger c_{R'+y,\uparrow}^\dagger \right) \right\rangle, \quad (13)$$

where $R' = R + rx$.

3 Results

Here, we work out the optimal wavelength of the stripe, assessing its conducting or insulating nature, for the hole doping $\delta = 1/8$, either fixing $t' = 0$ and varying the strength of the

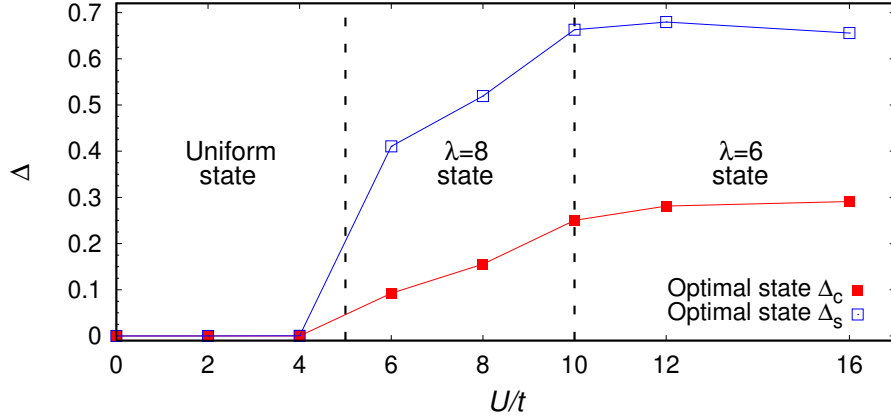


Figure 1: The variational parameters Δ_c (red full squares) and Δ_s (blue empty squares), for charge and spin modulations, see Eqs. (6) and (7). Results are shown for $t' = 0$, as a function of U/t . Data with $\lambda = 8$ and for the uniform case are reported for $L_x = 16$, while data with $\lambda = 6$ are shown for $L_x = 24$. At $U/t = 10$, where two solutions are degenerate, we show data for $\lambda = 6$.

Table 1: Energies per site (in unit of t) of the stripe state with $\lambda = 8$ and of the uniform state, for $U/t = 8$ and $t' = 0$, for different values of the lattice size $L = L_x \times 6$. The error bar on the energy is always smaller than 10^{-4} .

L_x	Energy striped state ($\lambda = 8$)	Energy uniform state
16	-0.7486	-0.7439
32	-0.7483	-0.7437
48	-0.7482	-0.7435
64	-0.7482	-0.7435

electron-electron interaction U or fixing U and varying the next-nearest-neighbor hopping t' . In the latter case, the values $U/t = 8$ and 12 are considered. The possible insurgence of superconductivity, also coexisting with stripes, is finally investigated.

3.1 Varying U/t with $t' = 0$

First of all, we analyze the case with $t' = 0$ and different values of U/t . We consider the variational energies for different stripe wavelengths λ , comparing them with the energy of a uniform state (which may still possess Néel order). For $U/t \lesssim 4$, all the striped wave functions are not stable, converging to the uniform state with vanishing parameters Δ_c and Δ_s . In addition, neither Néel order nor electron pairing is obtained in the auxiliary Hamiltonian of Eq. (4), indicating that the best state is a standard metal. For $6 \lesssim U/t \lesssim 8$, the best energy is obtained for $\lambda = 8$; instead, for $U/t \gtrsim 10$ (we did not consider values of the Coulomb interaction larger than $U/t = 16$) the optimal stripe has $\lambda = 6$. For $U/t \approx 10$, the energies of these two states are very close to each other. The variational parameters Δ_c and Δ_s for the optimal state are reported in Fig. 1, as a function of U/t . They are both finite where stripes

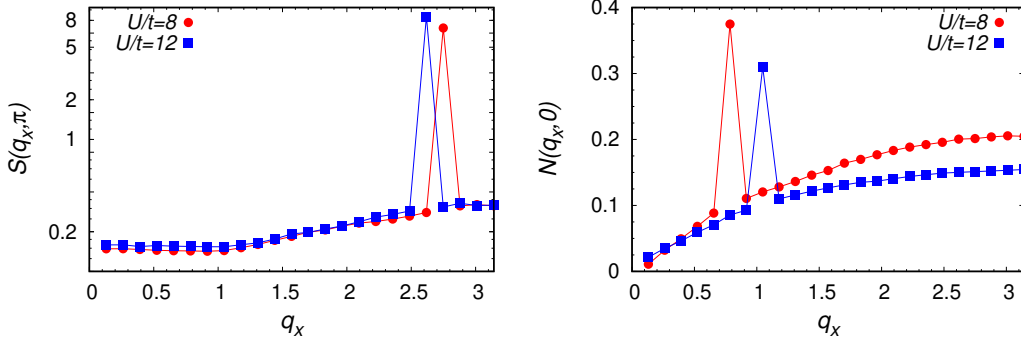


Figure 2: Left panel: Spin-spin correlation function $S(\mathbf{q})$ on a semi-log scale, as a function of q_x with $q_y = \pi$. Results are reported for $t' = 0$ and $L_x = 48$. The best variational state has $\lambda = 8$ at $U/t = 8$ (red circles) and $\lambda = 6$ at $U/t = 12$ (blue squares). Right panel: Same as in the left panel, but on a linear scale for the static structure factor $N(\mathbf{q})$ with $q_y = 0$.

are present, with the spin modulation being stronger than the charge one, while they collapse to zero for $U/t \lesssim 4$.

Then, we briefly discuss the dependence of the variational energies on the lattice size. In particular, we focus our attention on $U/t = 8$, where the lowest-energy state has a stripe with $\lambda = 8$. The variational energies of the striped wave function and the uniform one are reported in Table 1, for lattice sizes ranging from $L_x = 16$ to $L_x = 64$. The energies have only tiny variations going from small to large systems, indicating a very fast convergence to the limit $L_x \rightarrow \infty$. Therefore, the optimal state can be obtained comparing energies already on small sizes. By contrast, large clusters are necessary to discriminate between metallic and insulating properties, since this requires the evaluation of the small- q behavior of $N(\mathbf{q})$.

The actual presence of charge and spin order in the wave function can be directly detected in the static structure factors of Eqs. (11) and (12), as shown in Fig. 2. Here, clear peaks, diverging with the system size (not shown), are present, for $\mathbf{q} = (\frac{2\pi}{\lambda}, 0)$ in the charge correlations $N(\mathbf{q})$ and for $\mathbf{q} = (\pi(1 - \frac{1}{\lambda}), \pi)$ in the spin correlations $S(\mathbf{q})$. In Ref. [28], two of us suggested that stripes are driven by spins rather than charges. Then, the shortening of the stripe when increasing the electron-electron repulsion could be explained by noticing that the antiferromagnetic energy scale $J = \frac{4t^2}{U}$ increases when decreasing U/t , as long as the system remains sufficiently correlated (i.e., $U/t \gtrsim 4$), and that for longer stripes the number of nearest-neighbor antiparallel spins increases.

Let us now assess the metallic or insulating behavior of the optimal state, as it can be extracted from the small- q behavior of the static structure factor $N(\mathbf{q})$. In Fig. 3, we show $N(\mathbf{q})/q_x$ for the striped states at $U/t = 8$ and at $U/t = 12$. We observe that for $U/t = 8$ the behavior of $N(\mathbf{q})/q_x$ extrapolates to zero when the lattice size increases, compatibly with an insulating behavior. On the contrary, for $U/t = 12$, $N(\mathbf{q}) \approx q_x$ at small q_x , clearly indicating that the state is metallic. The latter result can be explained by the fact that the wavelength of the stripe is not commensurate with the doping, since an integer number of holes cannot be accommodated in the unit cell of the charge modulation.

Finally, we report that small but finite superconducting parameters Δ_x and Δ_y can be stabilized in the auxiliary Hamiltonian of Eq. (10) for $U/t \gtrsim 4$. However, they do not give rise to sizable pair-pair correlations $D(r)$, as defined in Eq. (13), see Fig. 4. Both the optimal

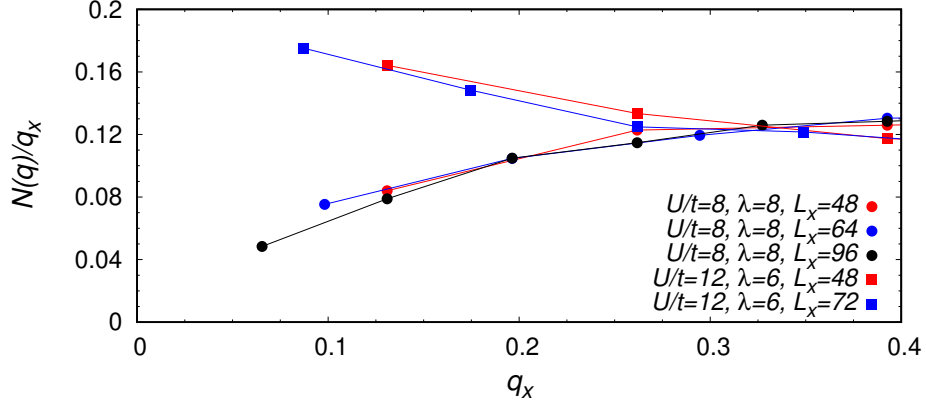


Figure 3: Static structure factor (divided by q_x) $N(\mathbf{q})/q_x$ as a function of q_x with $q_y = 0$. Data are reported for $t' = 0$ and different values of L_x . The optimal state has $\lambda = 8$ for $U/t = 8$ (circles) and $\lambda = 6$ for $U/t = 12$ (squares).

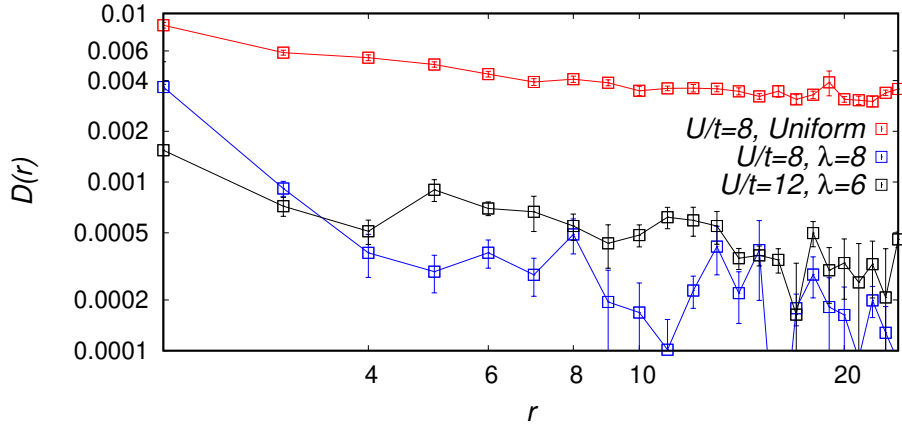


Figure 4: Pair-pair correlations $D(r)$ as a function of r for the optimal striped state with $\lambda = 8$ at $U/t = 8$ (blue squares), the one with $\lambda = 6$ at $U/t = 12$ (black squares), and the uniform state (not optimal) at $U/t = 8$ (red squares). Data are shown for $L_x = 48$ on a log-log scale.

striped state with $\lambda = 8$ at $U/t = 8$ and the one with $\lambda = 6$ at $U/t = 12$ show strongly suppressed pair-pair correlations with respect to the uniform case at $U/t = 8$ (that has a higher variational energy). Remarkably, the two striped states have a similar suppression in $D(r)$ even if one state is insulating and the other one is metallic. We mention that results for the striped states are shown for modulated pairings in the variational wave function, see Eq. (10), but the results are similar also imposing a uniform pairing.

3.2 Varying t'/t with $U/t = 8$ and 12

We fix now the value of U/t and vary t'/t . We start by considering $U/t = 8$, see Fig. 5. Here, both Δ_c and Δ_s are finite in a relatively large regime, i.e., for $-0.4 \lesssim t'/t \lesssim 0.25$. For

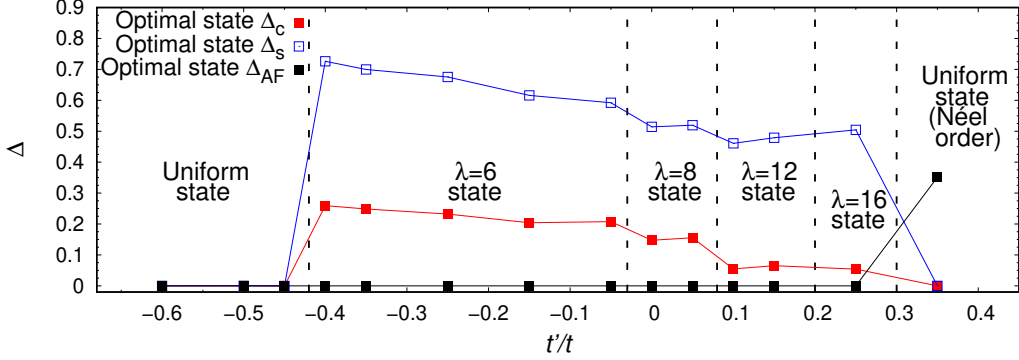


Figure 5: The variational parameters Δ_c (red full squares), Δ_s (blue empty squares), and Δ_{AF} (black full squares), see Eqs. (6), (7), and (8). Results are shown for $U/t = 8$ as a function of t'/t . Data with $\lambda = 8$ are reported for $L_x = 16$, with $\lambda = 6$ and 12 for $L_x = 24$, and with $\lambda = 16$ for $L_x = 32$; finally, data for the uniform cases are reported for $L_x = 16$.

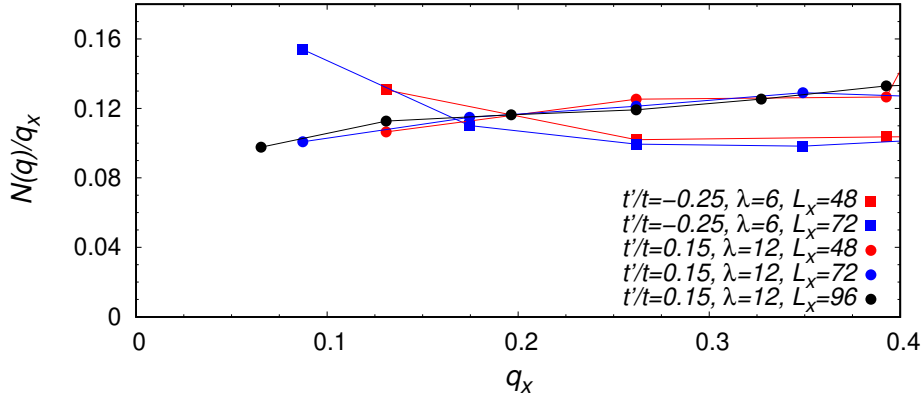


Figure 6: Static structure factor (divided by q_x) $N(\mathbf{q})/q_x$ as a function of q_x with $q_y = 0$. Results are reported for $U/t = 8$ at $t'/t = -0.25$ for the optimal striped state with $\lambda = 6$ (squares) and at $t'/t = 0.15$ for the optimal striped state with $\lambda = 12$ (circles). Different values of L_x are shown.

negative values of t'/t , the stripe wavelength reduces to $\lambda = 6$, until the optimal state becomes uniform, with no magnetic Néel order, for $t'/t \lesssim -0.45$. The transition is first order, with a clear jump in the values of Δ_c and Δ_s . The maximum energy gain between the striped state and the uniform one is reached for $t'/t \approx -0.25$, which is often considered to be a prototypical value for the cuprate family [33]. In this case, we have verified that the stripe with $\lambda = 6$ represents the best-energy solution also in two dimensional systems, e.g., on the $L = 24 \times 24$ cluster. For positive values of t'/t , the optimal λ increases first to $\lambda = 12$ and then to $\lambda = 16$, until the system becomes uniform again, but with antiferromagnetic Néel order. In this case, the transition is weakly first order. In general, a large value of $|t'/t|$ acts to frustrate the stripe pattern, with a striking difference between negative and positive values of t'/t ; while the former one gives rise to a uniform ground state, the latter one stabilizes a relatively strong Néel order (for very large values of $t'/t \approx 0.75$, we expect that Néel order is replaced by a

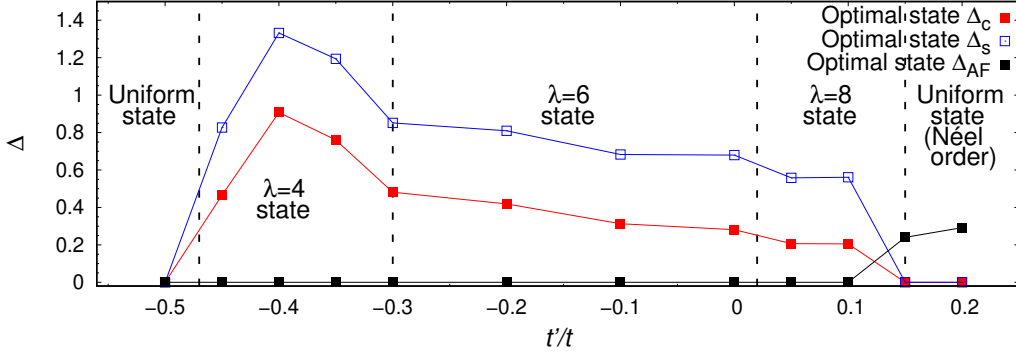


Figure 7: The same as in Fig. 5 but for $U/t = 12$. All data are shown for $L_x = 48$. At $t'/t = -0.3$ and at $t'/t = 0.15$, where two solutions are degenerate, we show data for $\lambda = 6$ and for the uniform state with Néel order, respectively.

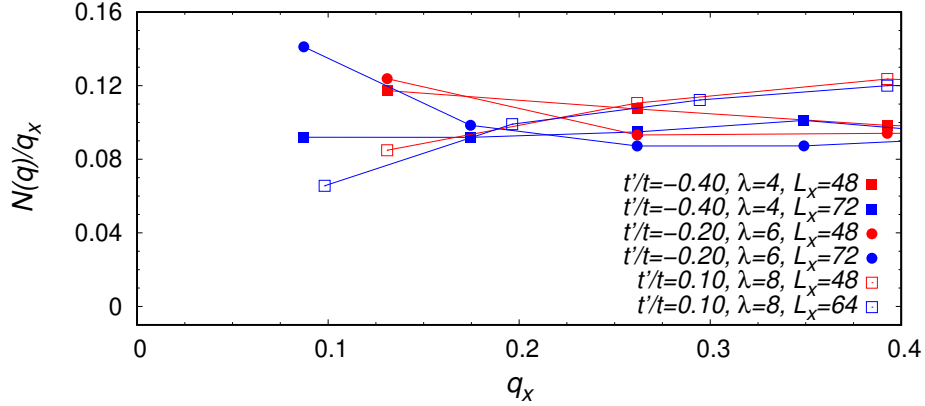


Figure 8: Static structure factor (divided by q_x) $N(\mathbf{q})/q_x$ as a function of q_x with $q_y = 0$. Results are reported for $U/t = 12$ at $t'/t = -0.4$ for the optimal striped state with $\lambda = 4$ (full squares), at $t'/t = -0.2$ with $\lambda = 6$ (full circles), and at $t'/t = 0.1$ with $\lambda = 8$ (empty squares). Different values of L_x are shown.

collinear order with pitch vector $\mathbf{K} = (\pi, 0)$ or $(0, \pi)$, as in the half-filled case with $\delta = 0$ [43]. The stability of Néel order up to large values of doping in the hole doped Hubbard model with positive values of t'/t (or equivalently in the electron doped Hubbard model with negative values of t'/t) has been discussed, for example, in Ref [48]. We remark that we cannot exclude the presence of longer stripes for positive values of t'/t : their detection would require very large clusters, being also difficult to distinguish them energetically from the uniform solution with Néel order. Finally, we stress that, for this value of U/t , the stripe with $\lambda = 4$ (recently obtained within tensor-network methods for $U/t = 10$ [36]) is not stabilized.

In Fig. 6, we show the behavior of $N(\mathbf{q})/q_x$ for the optimal states with $\lambda = 6$ at $t'/t = -0.25$ and for $\lambda = 12$ at $t'/t = 0.15$. Here, the results of the striped states are consistent with a metallic behavior, indicating again that a striped state is insulating only for particular values of its wavelengths, e.g., for $\lambda = 8$ at $\delta = 1/8$.

Finally, we want to assess the properties for a larger value of the electron-electron inter-

Table 2: Energy per site (in unit of t) for the best striped state and the uniform one, for $U/t = 12$, as a function of t'/t . Data are shown for $L_x = 48$. The error bar on the energy is always smaller than 10^{-4} .

t'/t	Energy best striped state	Energy uniform state
-0.5	-0.6258 ($\lambda = 4$)	-0.6261
-0.45	-0.6215 ($\lambda = 4$)	-0.6202
-0.4	-0.6208 ($\lambda = 4$)	-0.6162
-0.35	-0.6186 ($\lambda = 4$)	-0.6135
-0.3	-0.6171 ($\lambda = 6$ and 4)	-0.6118
-0.2	-0.6167 ($\lambda = 6$)	-0.6113
-0.1	-0.6193 ($\lambda = 6$)	-0.6147
0	-0.6254 ($\lambda = 6$)	-0.6227
0.5	-0.6309 ($\lambda = 8$)	-0.6283
0.1	-0.6375 ($\lambda = 8$)	-0.6355
0.15	-0.6448 ($\lambda = 8$)	-0.6447

action, i.e., $U/t = 12$. The main reason for doing this analysis is to verify whether stripes with $\lambda = 4$ may be stabilized or not. In fact, this is possible for sufficiently large and negative values of t'/t , see Fig. 7, where we report the variational parameters Δ_c and Δ_s for the optimal state, as a function of t'/t . In Table 2, we also show the energy of the best striped state and of the uniform one, as a function of t'/t . As observed for $U/t = 8$, the optimal stripe wavelength decreases for negative values of t'/t until a first-order transition to the uniform state takes place at $t'/t \approx -0.5$. The stripe with wavelength $\lambda = 4$ is then stabilized in the region $-0.45 \lesssim t'/t \lesssim -0.3$. Instead, for positive values of t'/t the stripe wavelength increases up to $\lambda = 8$ until the system becomes uniform (with Néel order) at $t'/t \approx 0.15$.

In Fig. 8, we show the behavior of $N(\mathbf{q})/q_x$ for the optimal states with $\lambda = 8$ at $t'/t = 0.1$, with $\lambda = 6$ at $t'/t = -0.2$, and with $\lambda = 4$ at $t'/t = -0.4$. Again, these results support the idea that the only insulating stripe is the one with $\lambda = 8$, which is commensurate with the doping level. In this case, $N(\mathbf{q})/q_x$ extrapolates to zero as the lattice size increases. On the contrary, in the other two cases $N(\mathbf{q})/q_x$ extrapolates to a finite value, indicating that the state is metallic.

Also for finite values of t'/t , small but finite superconducting parameters Δ_x and Δ_y can be stabilized in the auxiliary Hamiltonian of Eq. (10). However, as in the $t' = 0$ case, stripes do not coexist with sizable pair-pair correlations $D(r)$, see Fig. 9. Remarkably, the uniform state, both at positive and negative values of t'/t (with Néel order in the former case) displays superconducting correlations, which, however, are suppressed with respect to the uniform case at $t' = 0$, see Fig. 4. Still, they are much stronger than in the presence of stripes.

4 Conclusions

By means of the variational Monte Carlo method, we have investigated the stability of stripes in the Hubbard model at doping $\delta = 1/8$, as a function of the next-nearest neighbor hopping

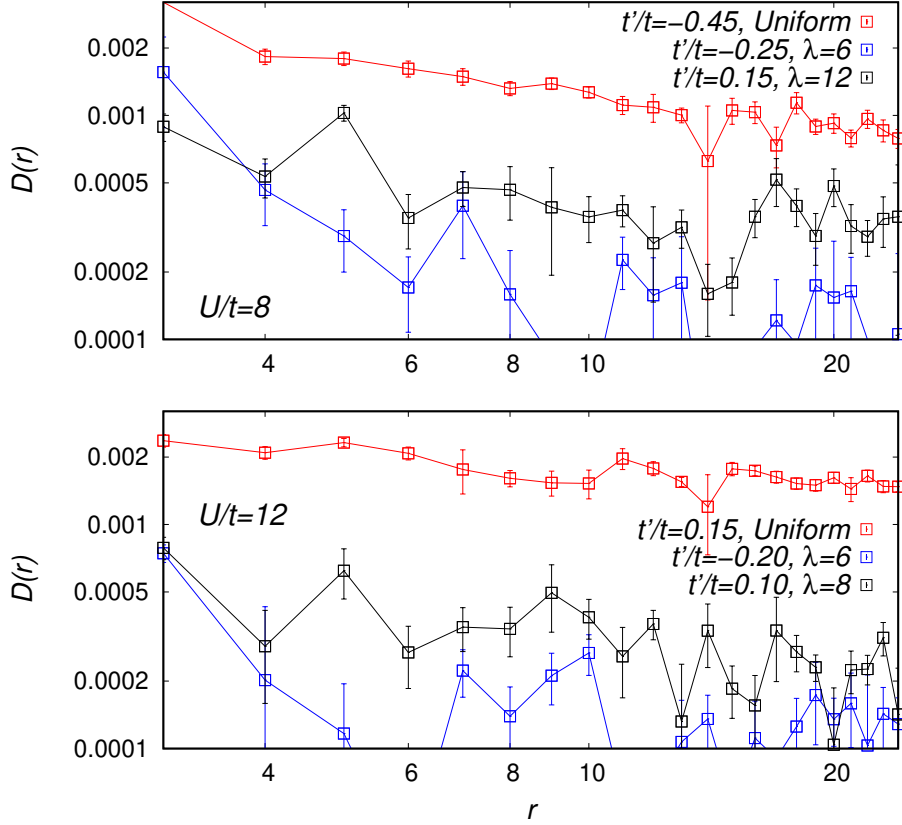


Figure 9: Pair-pair correlations $D(r)$ as a function of r . Lower panel: three optimal states at $U/t = 12$: the striped state with $\lambda = 6$ at $t'/t = -0.2$ (blue squares), the striped state with $\lambda = 8$ at $t'/t = 0.1$ (black squares), and the uniform state (with Néel order) at $t'/t = 0.15$ (red squares). Upper panel: three optimal states at $U/t = 8$: the striped state with $\lambda = 6$ at $t'/t = -0.25$ (blue squares), the striped state with $\lambda = 12$ at $t'/t = 0.15$ (black squares), and the uniform state at $t'/t = -0.45$ (red squares). Data are shown for $L_x = 48$ on a log-log scale.

t' and of the Coulomb repulsion U . In particular, we compared the uniform state (which possibly includes electron pairing and Néel order) with striped states with various wavelengths λ . The summary of our results is shown in Fig. 10. The present work extends our previous analysis [28], where we observed an insulating filled stripe with $\lambda = 8$ at doping $\delta = 1/8$, with $t' = 0$ and $U/t = 8$.

Firstly, we have shown that a sufficiently large Coulomb interaction is necessary to stabilize the stripes, since a weakly correlated metallic phase is present for $U/t \lesssim 4$. Instead, for $U/t \gtrsim 4$, the phase diagram is pervaded by striped states, whose wavelength depends upon the value of U/t . In general, we found a shortening of the stripe length when increasing U/t . This result may be associated to the corresponding weakening of the antiferromagnetic energy scale, since a longer stripe is closer to the standard antiferromagnetic Néel order, that maximally satisfies the antiferromagnetic energy scale.

Then, we observed that stripes are shorter for negative values of t'/t and become longer for

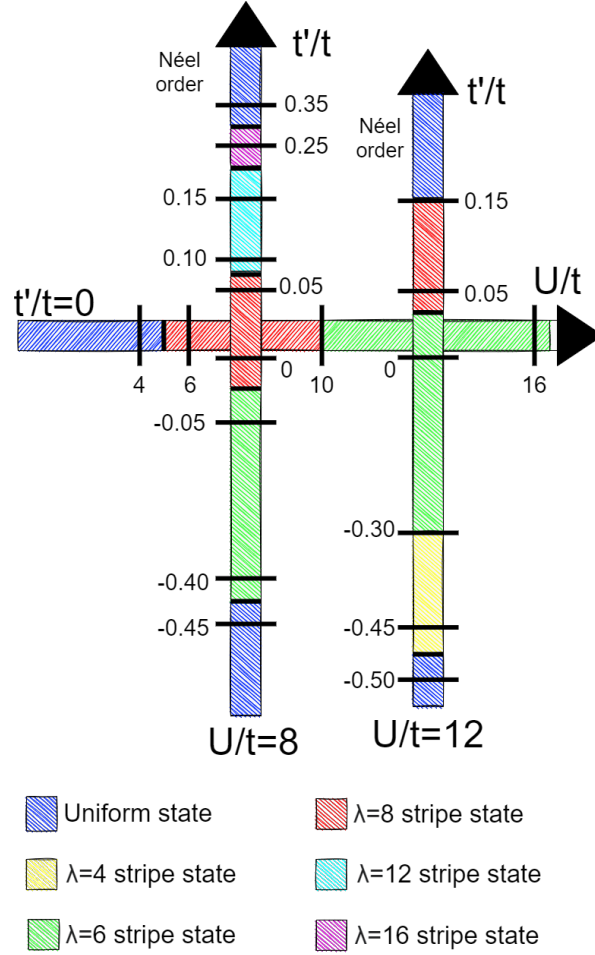


Figure 10: Schematic phase diagram as a function of U/t for $t' = 0$ and as a function of t'/t for $U/t = 8$ and $U/t = 12$.

positive values of it, as shown in Fig. 10, with the maximal energy gain between the striped case and the uniform one that is reached at $t'/t \approx -0.25$. We remark that stripes are present as long as the ratio $|t'/t|$ is not too large. The uniform ground state obtained for large enough $|t'/t|$ possesses Néel order for positive values of the ratio t'/t , while it has no spin order for negative values of it. We emphasize that the experimentally observed half-filled stripe with $\lambda = 4$ is stabilized only in the strongly correlated regime for negative values of t'/t .

Finally, we report that only the stripe with $\lambda = 8$ is insulating, since it is the only one that is commensurate with the hole doping. All the other striped states are metallic. Remarkably, despite their metallic nature, stripes seem do not ever coexist with superconductivity at doping $\delta = 1/8$, since pair-pair correlations are always strongly suppressed with respect to the uniform superconducting state.

Acknowledgments

We thank M. Grilli, R. Tateo, and A. Montorsi for useful discussions. Computational resources were provided by HPC@POLITO (<http://www.hpc.polito.it>).

References

- [1] J. Bednorz and K. Müller, *Possible high T_c superconductivity in the Ba-La-Cu-O system*, Z. Phys. B **64**, 189 (1986), doi:10.1007/BF01303701.
- [2] E. Dagotto, *Correlated electrons in high-temperature superconductors*, Rev. Mod. Phys. **66**, 763 (1994), doi:10.1103/RevModPhys.66.763.
- [3] P. Lee, N. Nagaosa and X.-G. Wen, *Doping a Mott insulator: Physics of high-temperature superconductivity*, Rev. Mod. Phys. **78**, 17 (2006), doi:10.1103/RevModPhys.78.17.
- [4] V. Emery, S. Kivelson and J. Tranquada, *Stripe phases in high-temperature superconductors*, Proceedings of the National Academy of Sciences **96**(16), 8814 (1999), doi:10.1073/pnas.96.16.8814.
- [5] V. Emery and S. Kivelson, *Frustrated electronic phase separation and high-temperature superconductors*, Physica C **209**, 597 (1993), doi:https://doi.org/10.1016/0921-4534(93)90581-A.
- [6] C. Castellani, C. Di Castro and M. Grilli, *Singular quasiparticle scattering in the proximity of charge instabilities*, Phys. Rev. Lett. **75**, 4650 (1995), doi:10.1103/PhysRevLett.75.4650.
- [7] J. Tranquada, B. Sternlieb, J. Axe, Y. Nakamura and S. Uchida, *Evidence for stripe correlations of spins and holes in copper oxide superconductors*, Nature **375**, 561 (1995), doi:10.1038/375561a0.
- [8] A. Bianconi, N. Saini, A. Lanzara, M. Missori, T. Rossetti, H. Oyanagi, H. Yamaguchi, K. Oka and T. Ito, *Determination of the local lattice distortions in the CuO₂ plane of La_{1.85}Sr_{0.15}CuO₄*, Phys. Rev. Lett. **76**, 3412 (1996), doi:10.1103/PhysRevLett.76.3412.
- [9] J. Hoffman, E. Hudson, K. Lang, V. Madhavan, H. Eisaki, S. Uchida and J. Davis, *A four unit cell periodic pattern of quasi-particle states surrounding vortex cores in Bi₂Sr₂CaCu₂O_{8+δ}*, Science **295**, 466 (2002), doi:10.1126/science.1066974.
- [10] C. Howald, H. Eisaki, N. Kaneko, M. Greven and A. Kapitulnik, *Periodic density-of-states modulations in superconducting Bi₂Sr₂CaCu₂O_{8+δ}*, Phys. Rev. B **67**, 014533 (2003), doi:10.1103/PhysRevB.67.014533.
- [11] G. Ghiringhelli, M. Le Tacon, M. Minola, S. Blanco-Canosa, C. Mazzoli, N. Brookes, G. De Luca, A. Frano, D. Hawthorn, F. He, T. Loew, M. M. Sala *et al.*, *Long-range incommensurate charge fluctuations in (Y,Nd)Ba₂Cu₃O_{6+x}*, Science **337**, 821 (2012), doi:10.1126/science.1223532.

- [12] R. Comin and A. Damascelli, *Resonant X-ray scattering studies of charge order in cuprates*, *Ann. Rev. Condens. Matter Phys.* **7**, 369 (2016), doi:10.1146/annurev-conmatphys-031115-011401.
- [13] R. Arpaia, S. Caprara, R. Fumagalli, G. De Vecchi, Y. Peng, E. Andersson, D. Betto, G. De Luca, N. Brookes, F. Lombardi, M. Salluzzo, L. Braicovich *et al.*, *Dynamical charge density fluctuations pervading the phase diagram of a Cu-based high- T_c superconductor*, *Science* **365**, 906 (2019), doi:10.1126/science.aav1315.
- [14] H. Miao, G. Fabbris, R. J. Koch, D. G. Mazzone, C. S. Nelson, R. Acevedo-Esteves, G. D. Gu, Y. Li, T. Yilmaz, K. Kaznatcheev, E. Vescovo, M. Oda *et al.*, *Charge density waves in cuprate superconductors beyond the critical doping*, *npj Quantum Materials* **6**, 31 (2021), doi:10.1038/s41535-021-00327-4.
- [15] A. Moodenbaugh, Y. Xu, M. Suenaga, T. Folkerts and R. Shelton, *Superconducting properties of $\text{La}_{2-x}\text{Ba}_x\text{CuO}_4$* , *Phys. Rev. B* **38**, 4596 (1988), doi:10.1103/PhysRevB.38.4596.
- [16] J. Axe, A. Moudden, D. Hohlwein, D. Cox, K. Mohanty, A. Moodenbaugh and Y. Xu, *Structural phase transformations and superconductivity in $\text{La}_{2-x}\text{Ba}_x\text{CuO}_4$* , *Phys. Rev. Lett.* **62**, 2751 (1989), doi:10.1103/PhysRevLett.62.2751.
- [17] J. M. Tranquada, *Spins, stripes, and superconductivity in hole-doped cuprates*, *AIP Conference Proceedings* **1550**(1), 114 (2013), doi:10.1063/1.4818402.
- [18] M. Qin, T. Schäfer, S. Andergassen, P. Corboz and E. Gull, *The Hubbard model: A computational perspective* (2021), 2104.00064.
- [19] S. White and D. Scalapino, *Stripes on a 6-leg Hubbard ladder*, *Phys. Rev. Lett.* **91**, 136403 (2003), doi:10.1103/PhysRevLett.91.136403.
- [20] G. Hager, G. Wellein, E. Jeckelmann and H. Fehske, *Stripe formation in doped Hubbard ladders*, *Phys. Rev. B* **71**, 075108 (2005), doi:10.1103/PhysRevB.71.075108.
- [21] C.-C. Chang and S. Zhang, *Spin and charge order in the doped Hubbard model: Long-wavelength collective modes*, *Phys. Rev. Lett.* **104**, 116402 (2010), doi:10.1103/PhysRevLett.104.116402.
- [22] B.-X. Zheng and G.-L. Chan, *Ground-state phase diagram of the square lattice Hubbard model from density matrix embedding theory*, *Phys. Rev. B* **93**, 035126 (2016), doi:10.1103/PhysRevB.93.035126.
- [23] B.-X. Zheng, C.-M. Chung, P. Corboz, G. Ehlers, M.-P. Qin, R. M. Noack, H. Shi, S. White, S. Zhang and G.-L. Chan, *Stripe order in the underdoped region of the two-dimensional Hubbard model*, *Science* **358**, 1155 (2017), doi:10.1126/science.aam7127.
- [24] D. Poilblanc and T. Rice, *Charged solitons in the Hartree-Fock approximation to the large- U Hubbard model*, *Phys. Rev. B* **39**, 9749 (1989), doi:10.1103/PhysRevB.39.9749.
- [25] J. Zaanen and O. Gunnarsson, *Charged magnetic domain lines and the magnetism of high- T_c oxides*, *Phys. Rev. B* **40**, 7391 (1989), doi:10.1103/PhysRevB.40.7391.

- [26] M. Kazushige, *Magnetism in La_2CuO_4 based compounds*, Physica C **158**, 192 (1989), doi:[https://doi.org/10.1016/0921-4534\(89\)90316-X](https://doi.org/10.1016/0921-4534(89)90316-X).
- [27] H. Schulz, *Domain walls in a doped antiferromagnet*, J. Phys. **50**, 2833 (1989), doi:[10.1051/jphys:0198900500180283300](https://doi.org/10.1051/jphys:0198900500180283300).
- [28] L. Tocchio, A. Montorsi and F. Becca, *Metallic and insulating stripes and their relation with superconductivity in the doped Hubbard model*, SciPost Phys. **7**, 21 (2019), doi:[10.21468/SciPostPhys.7.2.021](https://doi.org/10.21468/SciPostPhys.7.2.021).
- [29] S. Sorella, *The phase diagram of the Hubbard model by variational auxiliary-field quantum Monte Carlo* (2021), 2101.07045.
- [30] M. Qin, C.-M. Chung, H. Shi, E. Vitali, C. Hubig, U. Schollwöck, S. White and S. Zhang, *Absence of superconductivity in the pure two-dimensional Hubbard model*, Phys. Rev. X **10**, 031016 (2020), doi:[10.1103/PhysRevX.10.031016](https://doi.org/10.1103/PhysRevX.10.031016).
- [31] T. Vanhala and P. Törmä, *Dynamical mean-field theory study of stripe order and d -wave superconductivity in the two-dimensional Hubbard model*, Phys. Rev. B **97**, 075112 (2018), doi:[10.1103/PhysRevB.97.075112](https://doi.org/10.1103/PhysRevB.97.075112).
- [32] A. Darmawan, Y. Nomura, Y. Yamaji and M. Imada, *Stripe and superconducting order competing in the Hubbard model on a square lattice studied by a combined variational Monte Carlo and tensor network method*, Phys. Rev. B **98**, 205132 (2018), doi:[10.1103/PhysRevB.98.205132](https://doi.org/10.1103/PhysRevB.98.205132).
- [33] E. Pavarini, I. Dasgupta, T. Saha-Dasgupta, O. Jepsen and O. K. Andersen, *Band-structure trend in hole-doped cuprates and correlation with T_{cmax}* , Phys. Rev. Lett. **87**, 047003 (2001), doi:[10.1103/PhysRevLett.87.047003](https://doi.org/10.1103/PhysRevLett.87.047003).
- [34] E. Huang, C. Mendl, H.-C. Jiang, B. Moritz and T. Devereaux, *Stripe order from the perspective of the Hubbard model*, npj Quantum Materials **3**, 22 (2018), doi:[10.1038/s41535-018-0097-0](https://doi.org/10.1038/s41535-018-0097-0).
- [35] K. Ido, T. Ohgoe and M. Imada, *Competition among various charge-inhomogeneous states and d -wave superconducting state in Hubbard models on square lattices*, Phys. Rev. B **97**, 045138 (2018), doi:[10.1103/PhysRevB.97.045138](https://doi.org/10.1103/PhysRevB.97.045138).
- [36] B. Ponsioen, S. Chung and P. Corboz, *Period 4 stripe in the extended two-dimensional Hubbard model*, Phys. Rev. B **100**, 195141 (2019), doi:[10.1103/PhysRevB.100.195141](https://doi.org/10.1103/PhysRevB.100.195141).
- [37] H.-C. Jiang and T. Devereaux, *Superconductivity in the doped Hubbard model and its interplay with next-nearest hopping t'* , Science **365**, 1424 (2019), doi:[10.1126/science.aal5304](https://doi.org/10.1126/science.aal5304).
- [38] Y.-F. Jiang, J. Zaanen, T. Devereaux and H.-C. Jiang, *Ground state phase diagram of the doped Hubbard model on the four-leg cylinder*, Phys. Rev. Research **2**, 033073 (2020), doi:[10.1103/PhysRevResearch.2.033073](https://doi.org/10.1103/PhysRevResearch.2.033073).
- [39] C.-M. Chung, M. Qin, S. Zhang, U. Schollwöck and S. White, *Plaquette versus ordinary d -wave pairing in the t' -Hubbard model on a width-4 cylinder*, Phys. Rev. B **102**, 041106 (2020), doi:[10.1103/PhysRevB.102.041106](https://doi.org/10.1103/PhysRevB.102.041106).

- [40] F. Becca and S. Sorella, *Quantum Monte Carlo approaches for correlated systems*, Cambridge University Press (2017).
- [41] M. Capello, F. Becca, M. Fabrizio, S. Sorella and E. Tosatti, *Variational description of Mott insulators*, Phys. Rev. Lett. **94**, 026406 (2005), doi:10.1103/PhysRevLett.94.026406.
- [42] M. Capello, F. Becca, S. Yunoki and S. Sorella, *Unconventional metal-insulator transition in two dimensions*, Phys. Rev. B **73**, 245116 (2006), doi:10.1103/PhysRevB.73.245116.
- [43] L. Tocchio, F. Becca, A. Parola and S. Sorella, *Role of backflow correlations for the nonmagnetic phase of the $t-t'$ Hubbard model*, Phys. Rev. B **78**, 041101 (2008), doi:10.1103/PhysRevB.78.041101.
- [44] L. Tocchio, F. Becca and C. Gros, *Backflow correlations in the Hubbard model: An efficient tool for the study of the metal-insulator transition and the large- U limit*, Phys. Rev. B **83**, 195138 (2011), doi:10.1103/PhysRevB.83.195138.
- [45] J. LeBlanc, A. Antipov, F. Becca, I. Bulik, G.-L. Chan, C.-M. Chung, Y. Deng, M. Ferrero, T. Henderson, C. Jiménez-Hoyos, E. Kozik, X.-W. Liu *et al.*, *Solutions of the two-dimensional hubbard model: Benchmarks and results from a wide range of numerical algorithms*, Phys. Rev. X **5**, 041041 (2015), doi:10.1103/PhysRevX.5.041041.
- [46] A. Himeda, T. Kato and M. Ogata, *Stripe states with spatially oscillating d -wave superconductivity in the two-dimensional $t-t'-J$ model*, Phys. Rev. Lett. **88**, 117001 (2002), doi:10.1103/PhysRevLett.88.117001.
- [47] R. Feynman, *Atomic theory of the two-fluid model of liquid helium*, Phys. Rev. **94**, 262 (1954), doi:10.1103/PhysRev.94.262.
- [48] M. Aichhorn, E. Arrigoni, M. Potthoff and W. Hanke, *Antiferromagnetic to superconducting phase transition in the hole- and electron-doped Hubbard model at zero temperature*, Phys. Rev. B **74**, 024508 (2006), doi:10.1103/PhysRevB.74.024508.